Photoresponse of Zener tunneling junctions of Pb(Ti,Zr)O_3/SrTiO_3 at low temperature

Watanabe, Yukio
Department of Physics, Kyushu University

Okano, Motochika
Department of Physics, Kyushu University

出版情報：Journal of Applied Physics. 94 (11), pp.7187-7192, 2003-12-01. American Institute of Physics
バージョン：

Photoresponse of Zener tunneling junctions of $Pb(Ti,Zr)O_3/SrTiO_3$ at low temperature

Cite as: Journal of Applied Physics **94**, 7187 (2003); https://doi.org/10.1063/1.1625085
Submitted: 16 May 2003 . Accepted: 17 September 2003 . Published Online: 10 November 2003

Yukio Watanabe and Motochika Okano

Photoresponse of Zener tunneling junctions of $Pb(Ti,Zr)O_3/SrTiO_3$ at low temperature

Yukio Watanabe[a] and Motochika Okano[b]
Department of Physics, Kyushu University, Hakozaki 6-10-1, Higashiku, Fukuoka, Fukuoka 812-8581, Japan

(Received 16 May 2003; accepted 17 September 2003)

Temperature (T) dependent current–voltage (IV) characteristics of epitaxial $Pb(Ti,Zr)O_3/SrTiO_3$ heterojunctions exhibiting the characteristics of Zener tunneling are measured in the dark and in the light. Ultraviolet light is found to induce a prominent photovoltaic effect at all T down to at least 50 K, while the open circuit voltage increases with decreasing T. In the dark the reverse bias current increases with decreasing T. In the light the reverse bias current at low T is a superposition of a photovoltaic current and a small component that is identical to the reverse bias current in the dark. These observations indicate that the anomalous T dependence of the reverse bias current in the dark is attributable to the tunneling from the $Pb(Ti,Zr)O_3$ band to the $SrTiO_3$ band. Additionally, short pulse voltages modulate the tunneling current, which is retained. © *2003 American Institute of Physics.* [DOI: 10.1063/1.1625085]

I. INTRODUCTION

Current conduction through oxide films and their heterostructures is intensively investigated to understand their basic properties and explore a wide range of applications, because of their diverse functionalities.[1] Examples are *n*- and *p*-type transparent conductors (*p*: hole carrier, *n*: electron carrier)[2] and their *pn* junctions,[3,4] e.g., for thermoelectric power generators[5] and spin electronics.[6] In such *pn* junctions, Nb-doped $SrTiO_3$ ($SrTiO_3$:Nb), which is a ferroelectric/paraelectric material, is frequently used as an *n*-type semiconductor.[3,5,7]

On the other hand, the properties of macroscopic ferroelectrics are mostly understood well by regarding it as an insulator. In mesoscopic and nanometer-scale ferroelectrics, however, free carriers play a fundamental role in determining the electric properties, because the electrostatics at the surface is of crucial importance. Indeed, the properties of ferroelectrics as semiconductors have been investigated, but the reported characteristics have been different from those of conventional semiconductors.[8] Recently, epitaxial ferroelectric heterostructures have been intensively studied, and the properties comparable to conventional semiconductors have been reported.[9]

Deep level transient spectroscopy (DLTS), x-ray photoemission spectroscopy (XPS), and the dependence of conductivity on the donor doping[10–13] show that undoped $Pb(Ti,Zr)O_3$ (PZT) thin films are *p* type at room temperature (RT), which is attributed to lead vacancies.[14] Such semiconductivity is conventionally regarded as extraneous, and ferroelectric thin films and their heterostructures are considered to be insulating at low temperatures (T); diodes of these materials are considered unusable at low T. The present article demonstrates a substantial photoresponse of *p*-PZT/*n*-$SrTiO_3$:Nb junctions at cryogenic T and suggests the prospect of ferroelectric heterostructures as a class of semiconductor heterostructures.

Furthermore, an anomalous current conduction increasing with decreasing T through PZT/$SrTiO_3$:Nb junctions has been reported.[15] This conduction is attributed to tunneling conduction through a *pn* junction, based on the low threshold voltage, the shape of the IV curves and its dependence on T, the impurity doping densities, the PZT layer thickness, and the choice of materials.

On the other hand, avalanche breakdown is one of the typical breakdown processes of *pn* diodes,[16,17] but is ignored in the previous paper.[15] For conventional semiconductors, the threshold voltage of avalanche breakdown is, typically, larger than $4E_g$ (E_g: band gap), whereas the observed threshold voltage is $0.3-0.8E_g$. In addition, the shape of the observed current–voltage (IV) characteristics is incompatible with avalanche breakdown.[18]

Nonetheless, these textbook criteria change by several factors.[19] Moreover, the threshold voltage of avalanche breakdown deceases usually with decreasing T,[20] which may be an alternate interpretation of the observed anomalous T dependence of the IV characteristics. On the other hand, the tunneling conduction through *pn* junctions of conventional semiconductors is relatively independent of T.[21]

By utilizing the distinct difference in their optical response, we can distinguish between avalanche breakdown and tunneling. Namely, the threshold voltage of avalanche breakdown is theoretically and experimentally shown to be extremely sensitive to illumination as utilized in avalanche photodiodes,[22] but that of tunneling is not.[23] The results below fortify the previous conclusion that the anomalous conduction is due to tunneling through an oxide *pn* junction.[15]

II. EXPERIMENT

C-axis oriented PZT and $Pb_{0.95}La_{0.05}Ti_{0.8}Zr_{0.2}O_3$ (PLZT) films are epitaxially grown on 0.5 wt% Nb-doped [001]

[a]Electronic mail: ynab7scp@mbox.nc.kyushu-u.ac.jp
[b]Present address: Toshiba Corp.

$SrTiO_3$ (STON) substrates by pulse laser deposition and are 150–400 nm thick. The lattice mismatch between the PZT films and the STON substrates is 1%. The STON substrates are estimated to have a donor density N_D of 5×10^{19} cm^{-3}. Pt and Au films with surface area from 0.1 to 1 mm^2 and thickness of 20–100 nm are the top electrodes. The bottom electrodes having large surface areas are formed on STON by silver paste. The effect of the contact resistance is invisible in the current–voltage (IV) characteristics in the dark, whereas it may be slightly visible under an intense ultraviolet (UV) light.

All measurements were performed in vacuum below 1×10^{-6} Torr. We obtained T-dependent IV characteristics by reaching first a fixed T, then, measuring IV curves in the dark and in the light, and moving to the next T. The voltage polarity was defined at the top metal electrode, and the scan time was 3.5 min for one cycle of IV curve (0 V $\rightarrow$maximum V$\rightarrow$0 V$\rightarrow$minimum V$\rightarrow$0 V). The IV characteristics measured at least twice for each set of measurement parameters confirmed an excellent reproducibility and the absence of irreversible changes. As a white light source we used a florescent light and as a UV light source a 150 W Hg–Xe lamp with a heat-absorption glass filter and color filters; its spectral energy peaks at 3.3 eV, i.e., near the band-gap energy of PZT and STON. IV characteristics changed gradually in the UV light. Therefore, the photoresponse was measured in a quasistable state that was achieved in 20–30 s after irradiation. The results in Figs. 1–5 are of the same electrode on the same PZT (200-nm-thick)/STON sample.

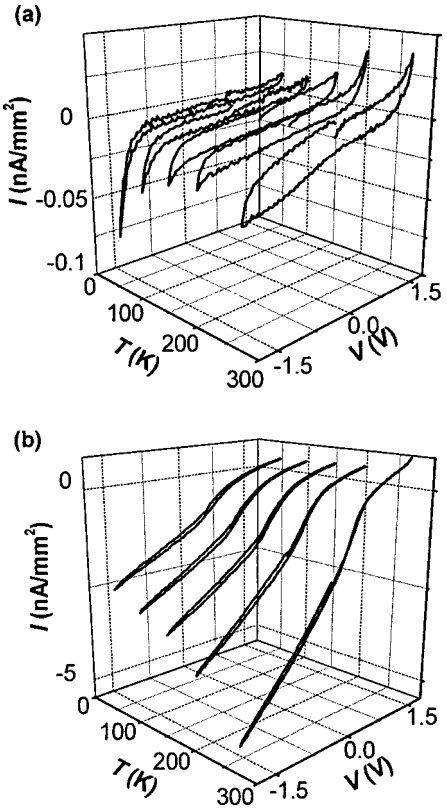

FIG. 1. IV characteristics of a PZT/STON junction at 50, 100, 150, 200, and 270 K ($|V| \leqslant 1.8$ V) in the dark (a) and in the UV light (b).

III. RESULTS

A. *IV* characteristics in the dark and intense light

Figure 1 shows the T dependence of IV characteristics in the dark and in the UV light. The IV characteristics at 270 K in Fig. 1(a), especially the polarity of the forward bias, are consistent with a junction of a p-type (PZT) and an n-type semiconductor (STON). Here, the formation of a pn junction by PZT and STON is supported also by the other results.[9,15,24] In the dark, the forward bias current diminishes with decreasing T. Contrarily, the reverse bias current grows with decreasing T to at least 20 K and exhibits IV characteristics of Zener tunneling at low T. Few irreversible changes of these properties are observed during temperature cycling between 20 and 290 K. We call this reverse bias dark current the ''Z component.''

The previous paragraph, the discussions in Refs. 15 and 24, and the following show that the conduction is limited by the PZT/STON interface. The series resistance of the metal contacts (M), the bulk part of the PZT film, and the PZT/STON interface is expected to limit the conduction through the M/PZT/STON/M′ (M, M′: metal). The forward bias polarity and the T dependence of the M/p-PZT and the n-STON/M′ contact are opposite to those in Fig. 1(a). Therefore, these contacts are secondary current-blocking parts. Additionally, the IV characteristics are almost independent of M. The bulk part of the PZT should exhibit no diode behavior or no conductance increasing with decreasing T. Consequently, the PZT/STON interface remains as the sole candidate compatible with Fig. 1(a).

UV light of 50 mW/cm^2 induces a drastic change in the IV characteristics in the entire T range down to at least 50 K [Fig. 1(b)]. Especially, it generates current, which is seen as the negative shift of the IV curves. Identification of the conduction mechanisms for such drastically changed IV characteristics requires supplementary data. Therefore, we examine first the response to the white light.

B. *IV* characteristics in weak light

Figure 2 shows a photoresponse to white light of 0.3 mW/cm^2. Optical enhancement of the reverse bias current is evident at 290 K, which warrants that the white light has an energy density sufficient to detect the optical effect on an avalanche breakdown, if it exists.

The observed photoresponse should be compared with typical IV characteristics of a photovoltaic effect and/or an avalanche breakdown (Fig. 2). In Figs. 2(a) and 2(b), the difference between the current at -1.8 V in the dark and in the light, is almost the same as the difference at -1.5 V. This observation and the T dependence in Fig. 3 signify that the illumination shifts little the threshold of the Z component; besides, this conclusion is confirmed by the estimation of the threshold voltage by the curve fitting to the IV curves in Fig. 2(b). These observations are consistent with the view that the observed photoresponse is due to a photovoltaic effect but not to a photoresponse of avalanche breakdown.

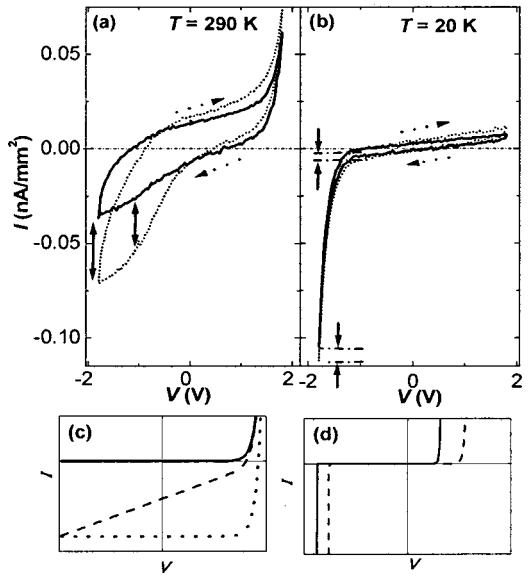

FIG. 2. (a)(b) Comparison of the IV curves in the dark (solid lines) and under the white light of 0.3 mW/cm^2 (dotted lines). The solid arrows show the difference between the current in the dark and in the light (at -1.5 and -1.8 V). The single arrows in Figs. 2, 4, and 6 indicate the direction of the voltage scan. (c) Ideal and nondeal photovoltaic characteristics: IV curves of an ideal *pn* junction in the dark (solid lines) and in the light (dotted lines) vs a nonideal IV curve (dashed lines). (d) Ideal avalanche breakdown in the dark (solid lines) and the light (dotted lines). The vertical shift of the IV curve due to the photovoltaic effect is invisible, because the shift is much smaller than the avalanche current.

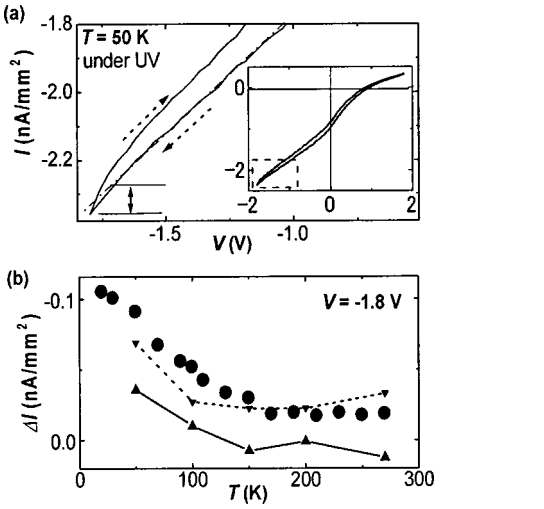

FIG. 4. (a) IV curve in the UV light enlarged from the inset that is reproduced from Fig. 1(b). The linear curve fitting to the data between -1 and -1.65 V is shown by the dash dot lines. The solid arrow (↕) shows the discrepancy (ΔI) between the data and the fitting at -1.8 V, explaining the procedure of extracting the "Z component." (b) T dependence of the Z-component ΔI obtained by this procedure (▲). The dotted lines with ▼ and the solid circles ● are the replots of the dark current at -1.8 V in Figs. 1(a) and 3, respectively.

C. Photovoltaic effect

Returning to Fig. 1(b), we see that UV light increases the reverse bias current drastically, e.g., at -1 V, by three orders of magnitude. As most easily confirmed in the inset of Fig. 4(a), the current is negative also at the positive bias, which confirms that the photoresponse in Fig. 1(b) is essentially a photovoltaic effect. Here, the deviation of the IV characteristics from those of an ideal photovoltaic effect is probably due to the carrier generation–recombination processes at the junction.[25]

The marked photovoltaic effect results primarily from the band structure of the PZT/STON junctions and the well-defined interface. The mechanism that permits the conduction of the substantial photovoltaic current despite the high dark resistance of the PZT at low T is presumably its photoconductivity.

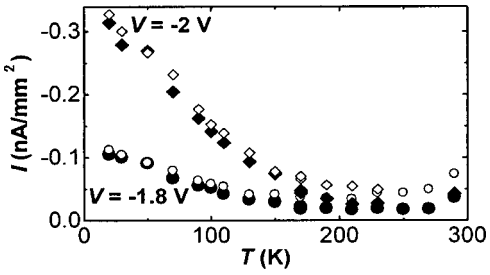

FIG. 3. (a) T dependence of the dark current (●◆) and the current in the white light (○◇). The circles ●○ ($V=-1.8$ V) and the diamonds ◆◇ ($V=-2$ V) represent the data from two independent series of experiments. The duplicate data points at 170 K (◆◇) are the data during cooling and heating.

D. Z component in photovoltaic current

Next, we focus on the Z component in Fig. 1. The procedure of the extraction of the Z component as the deviation of the IV curve from a linear curve fitting is shown in Fig. 4(a), which is a magnified view of its inset. The T dependence of the Z component in the UV light extracted by this procedure agrees with the T dependence of the Z component in the dark, except for a uniform shift of the current density [Fig. 4(b)].

We examine this finding by comparing rigorously the Z components in the UV light and in the dark. This is complicated by the hystereses of the IV curves: the absolute current density $|I|$ is higher for the increasing absolute voltage $|V|$ than for the decreasing $|V|$. The hystereses decrease by reducing the sweep speed, suggesting that they are due to the dielectric relaxation. Here, the steps of $V(dV)$ and $t(dt)$ are kept constant during each IV characteristics measurement. Therefore, we use the current density $I=[I^+(V)+I^-(V)]/2$ that contains little dielectric relaxation current $C dV/dt$ (C: capacitance, t: time), where $I^+(V)$ is the current density for the increasing $|V|$ and $I^-(V)$ for the decreasing $|V|$.

Figure 5(a) shows the IV curves extracted from Fig. 1(a) through this procedure.[26] We remove, also, dielectric relaxation components from the data in Fig. 1(b) in the same manner. Then, with a straight line we fit the linearly changing section of the resulting curves, e.g., between -1.2 and -0.3 V. Using the obtained fitting parameters, we subtract the linearly changing component as a photovoltaic and a generation–recombination component to obtain Fig. 5(b).

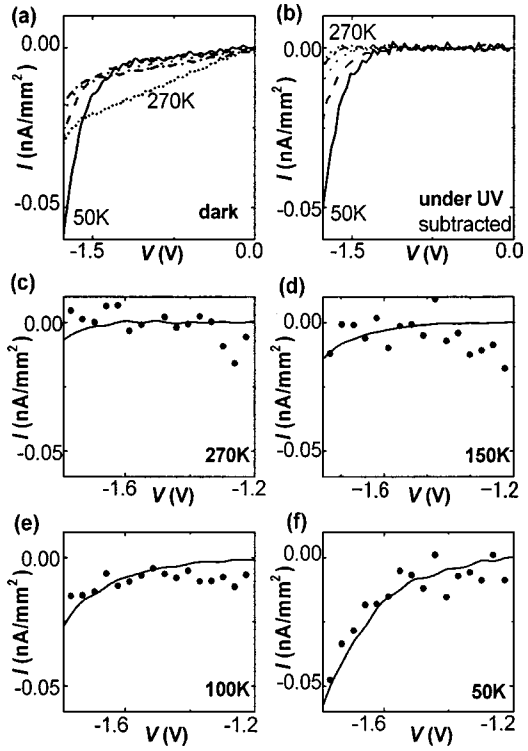

FIG. 5. (a) *IV* curves in the dark extracted from Fig. 1(a) by subtracting the capacitive contributions. (b) *IV* curves in the UV light extracted from Fig. 1(b) by subtracting the capacitive contributions and the linearly changing component. In (a) and (b), the short dotted lines: 270 K, the dash-dot lines: 200 K, the dotted lines: 150 K, the dashed lines: 100 K, the solid lines: 50 K. (c)–(f) Comparison of *IV* characteristics in the dark (solid lines) and the UV light (solid circles) from (a) and (b). In these plots, the linearly changing components in (a) are also subtracted.

By comparing Figs. 5(a) and 5(b), we find that the extracted *IV* curves in the UV light resemble closely those in the dark in the overall *T* dependence, shape, and current density. For a closer comparison, the linearly changing component in the dark [Fig. 5(a)], which is evident at 270 K, is also subtracted, because it is presumably a generation–recombination current. The resulting *IV* characteristics should represent pure *Z* components, which are shown by the solid lines in Figs. 5(c)–5(f). Now, we can compare them rigorously with the replots of Fig. 5(b), shown by the filled circles. Although the *IV* characteristics are slightly noisy, probably owing to UV light-enhanced generation–recombination noise, overall agreement is satisfactory, especially at 50 K. Here, the comparison at this *T* should be the most important, because the *Z* component is manifested at low *T*. These analyses confirm that the *Z* component is unaffected even by an intense UV light. Namely, the current density or the threshold is unchanged. Therefore, the avalanche breakdown is excluded from the origin of the *Z* component.

The photoresponse of an ideal tunneling diode is a superposition of a tunneling process and a photovoltaic effect, and the resulting *IV* curve is the vertical shift of the *IV* curve of the tunneling diode.[23] We conclude that this is what we see in Fig. 1(b). It should be emphasized that the threshold voltage of the *Z* component is relatively independent of the PZT thickness of 150–400 nm. This observation and the unfeasibility of the tunneling through the distance of over 200 nm indicate that a direct tunneling from the metal electrode to the STON is excluded. Therefore, the photoresponse discussed above and the reported properties of the shape of the *IV* curves, the material, doping, and thickness dependence,[15] indicate consistently the tunneling from the PZT valence band to the STON conduction band. Especially, the *T* dependence suggests that this tunneling is not phonon assisted. The insensitivity of the *Z* component to the UV light, which can activate traps or defects, suggests that the tunneling is neither via traps nor via defects, but is direct. Having assigned the observed photoresponse to a photovoltaic effect, its *T* dependence is characterized by the open circuit voltage of 0.8–1.0 V that increases with decreasing *T*.

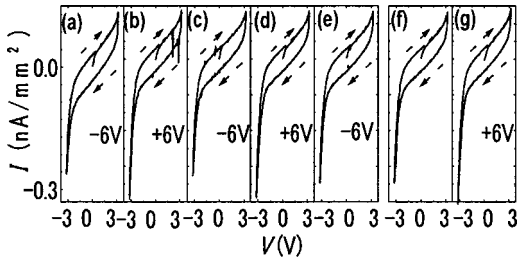

FIG. 6. Pulse voltage control of the *IV* characteristics of a PLZT(La-doped)/STON diode at 20 K and its retention. (b), (d), and (g) after +6 V 10 μs pulse; (a), (c), and (e) after −6 V 10 μs pulse; and (f) after holding of 3 h after the measurement of (e). The threshold voltage for the *Z* component increases by La doping as in Ref. 15.

E. Pulse voltage control of the tunneling current

It would be intriguing to explore the unique property of the present tunneling diode. At low *T* both spontaneous polarization (P_S) and charge injection can induce a persistent change of the band bending.[9,27] Therefore, pulse voltage can control the Zener tunneling through the PZT/STON junction. The diode shows fair polarization hysteresis loops, and the 5 μs voltage pulses of ±6 V at 170 K change the *Z* component by 20%.

We have performed similar measurements on a PLZT/STON sample that conducts less tunneling current to obtain a larger P_S switching. The 10 μs pulses of ±6 V modulate the diode characteristics at 20 K. All the *IV* curves in Fig. 6, except for Fig. 6(f) are measured immediately after one switching pulse. The results demonstrate the pulse control of the tunneling current and the retention of the modulation for at least 3 h.

These experiments reconfirm that the conduction is controlled by the region that is strongly influenced by either P_S or charge injection, i.e., the PZT/STON interface.[9] The conductance change of 20% is small. Here, we have applied only low voltage short pulses to suppress a charge injection effect. These pulses are probably able to switch P_S only partially, because the coercive force increases with decreasing *T*. This interpretation is consistent with an increase of the conductance modulation at 100 K that is 40% for 5 μs voltage pulses of ±6 V and is retained for at least 10 h.

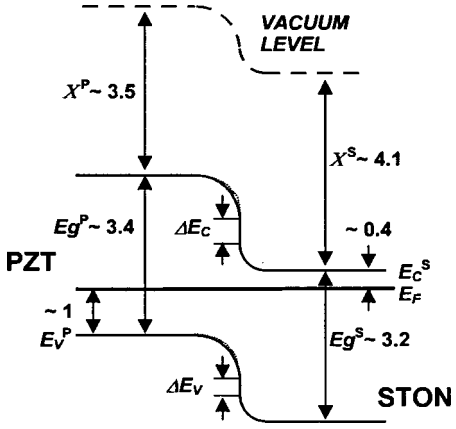

FIG. 7. Tentative band diagram of PZT/STON with quantities in the unit of eV. E_g, X, E_C, E_V, and E_F are the band gap and the electron affinity, the bottom of the conduction band, the top of the valence band, and the Fermi level, respectively. The superscripts S and P attached to E_g, X, E_C, and E_V indicate that these quantities are of STON and PZT, respectively. The discontinuities of the band edge ΔE_C and ΔE_V are given by $\Delta E_C = X^S - X^P \approx 0.6$ eV and $\Delta E_V = E_g^S + X^S - X^P - E_g^P \approx 0.4$ eV. The dotted lines show the possible change induced by the spontaneous polarization or the injected charges.

IV. DISCUSSION

A. Band diagram

It would be interesting to discuss the present results based on a band diagram. Figure 7 shows a band diagram of the PZT/STON at RT using the parameters in Refs. 11–13. The diagram is depicted by assuming an Anderson model,[28] which is a proper approximation because of good lattice and chemical matching of PZT with STON and a well-defined interface. The diagram supports a *pn* junction formation and is consistent with the observed photovoltaic characteristics. Additionally, the diagram predicts a possibility of Zener tunneling at applied voltages below -1.5 V, which is close to the observed threshold voltage.

As discussed in Ref. 15, as T decreases the Fermi level E_F is expected to approach the bottom of the STON conduction band E_C^S and the top of the PZT valence band E_V^P. This accounts for the decrease of the Zener tunneling threshold voltage with decreasing T. Additionally, the T dependence of E_F explains the increase of open circuit voltage with decreasing T.

B. Other issues

First, the open circuit voltage in Fig. 1(b) is reduced by a hump structure. We speculate that the hump structure is due to a generation–recombination process or indirect tunneling enhanced by optically increased active traps in the depletion layer.[29] Second, the threshold voltage for the tunneling current depends on preparation conditions of PZT such as growth temperature; the junctions with nominally the same PZT composition exhibit sometimes different threshold voltages for tunneling. Possible causes are mechanical stress as reported for InSb diodes[30] and variation of the depletion layer width by dislocations. Third, in the present experiment, a half area of the top electrode was covered by an indium dot and was unexposed to illumination. Nevertheless, it would be clear that the above results and the conclusions are unchanged except for the efficiency of the photovoltaic effect.[31,32] Fourth, the spectral peak energy of the UV source (3.3 eV) is slightly lower than the band-gap energy of PZT at RT (3.4 eV). Therefore, the decrease of the photovoltaic current with decreasing T is at least partly due to the increase of the band-gap of PZT with decreasing T.

V. CONCLUSIONS

In summary, the present article reports the photoresponse of the PZT/STON ferroelectric *pn* junctions down to 20 K. These junctions exhibit a substantial photoresponse at cryogenic T. The reverse bias current in the dark increases with decreasing T and is called the Z component. This component is attributable to the band-to-band tunneling through the PZT/STON *pn* junction. By doping PZT further, the low voltage operation and the prominent photoresponse at low T reported here can be useful in space, if combined with the mechanical strength, radiation hardness, and ferroelectricity, such as pyroelectric infrared detection. The present results may also have implications for the surface and the finite size effect of ferroelectrics.[33]

ACKNOWLEDGMENTS

This study is motivated by discussions at Bell Laboratories, Murray Hill. The authors acknowledge the support of a grant-in-aid from the ministry of education (Grant No. 12134208).

[1] K. C. Kao and W. Hwang, *Electrical Transport in Solids* (Pergamon, Oxford, U.K., 1981).
[2] H. Kawazoe, M. Yasukawa, H. Hyodo, M. Kurita, H. Yanagi, and H. Hosono, Nature (London) **389**, 939 (1997); V. B. Chougule and S. H. Pawar, Solid State Commun. **48**, 17 (1983).
[3] Y. Xu, C. J. Chen, R. Xu, and J. D. Mackenzie, J. Appl. Phys. **67**, 2985 (1990).
[4] E. Traversa, A. Bearzotti, M. Miyayama, and H. Yanagida, J. Mater. Res. **10**, 2286 (1995).
[5] I. Matsubara, R. Funahashi, T. Takeuchi, S. Sodeoka, T. Shimizu, and K. Ueno, Appl. Phys. Lett. **78**, 3627 (2001).
[6] H. Tanaka, K. Betsuyaku, H. K. Yoshida, and T. Kawai, Solid State Commun. **122**, 677 (2002).
[7] B. Reihl, J. G. Bednorz, K. A. Müller, Y. Jugnet, G. Landgren, and J. F. Morar, Phys. Rev. B **30**, 803 (1984); Z. Sroubek, Solid State Commun. **7**, 1561 (1969); J. F. Schooley, R. J. Soulen, Jr., and C. S. Koonce, *ibid.* **7**, 1077 (1969); Z. Sroubek and F. Kube, *ibid.* **12**, 767 (1973).
[8] V. Yarmarkin, B. Gol'tsman, M. Kazanin, and V. Lemanov, Phys. Solid State **42**, 522 (2000); W. T. H. Koch, R. Munser, W. Ruppel, and P. Würfel, Solid State Commun. **17**, 847 (1975).
[9] Y. Watanabe, Phys. Rev. B **59**, 11257 (1999); Y. Watanabe and M. Okano, Appl. Phys. Lett. **78**, 1906 (2001).
[10] S. Iakovlev, C.-H. Solterbeck, and M. Es-Souni, Appl. Phys. Lett. **81**, 1854 (2002); R. C. Ibrahim, T. Horiuchi, T. Shiosaki, and K. Matsushige, Jpn. J. Appl. Phys., Part 1 **37**, 6060 (1998).
[11] P. F. Baude, C. Ye, and D. L. Polla, Appl. Phys. Lett. **64**, 2670 (1994).
[12] B. Nagaraj, S. Aggarwal, T. K. Song, T. Sawhney, and R. Ramesh, Phys. Rev. B **59**, 16022 (1999).
[13] J. F. Scott, Jpn. J. Appl. Phys., Part 1 **38**, 2272 (1999).
[14] R. Gerson and H. Jaffe, J. Phys. Chem. Solids **24**, 979 (1963). It may be natural to assume PZT films as *n* type because of oxygen vacancies. However, the oxygen vacancies are found to increase the lead vacancies that work as acceptors.
[15] Y. Watanabe, Phys. Rev. B **57**, R5563 (1998).
[16] S. M. Sze, *Physics of Semiconductor Devices* (Wiley, New York, 1981); J. M. Early, Proc. IRE **40**, 1401 (1952).
[17] The old commercial Zener diodes and many of recent ones are in fact not

tunneling diodes but avalanche diodes. The wrong naming originates from the misinterpretation of the avalanche breakdown of the *pn* diodes as the Zener tunneling in early days.

[18] For example, E. V. Bogdanov, N. B. Brandt, L. S. Fleyshman, and V. L. Popov, Solid State Commun. **53**, 947 (1985); S.-L. Jang and K.-L. Chern, Solid-State Electron. **35**, 615 (1992); F. Yan, J. H. Zhao, and G. H. Olsen, *ibid.* **44**, 341 (2000).

[19] For example, T. Tomimatsu, Appl. Phys. Lett. **35**, 65 (1979).

[20] For example, T. Abe, H. Ishikura, N. Fukuda, Z. Aung, M. Adachi, H. Kasada, and K. Ando, J. Cryst. Growth **214/215**, 1134 (2000); F. Yan, C. Qin, J. H. Zhao, M. Bush, G. Olsen, B. K. Ng, J. P. R. David, R. C. Tozer, and M. Weiner, Solid-State Electron. **47**, 241 (2003).

[21] J. V. Morgan and E. O. Kane, Phys. Rev. Lett. **3**, 466 (1959).

[22] For example, L. A. Kosyachenko, I. M. Rarenko, S. Weiguo, and Lu Z. Xiong, Solid-State Electron. **44**, 1197 (2000); A. Pauchard, P.-A. Besse, M. Bartek, R. F. Wolffenbuttel, and R. S. Popovic, Sens. Actuators A **82**, 128 (2000).

[23] R. F. Adams and R. L. Rosenberg, Appl. Phys. Lett. **12**, 414 (1969).

[24] M. Okano, D. Sawamura, and Y. Watanabe, Jpn. J. Appl. Phys., Part 1 **37**, 1501 (1998).

[25] For example, N. S. Saricifti, D. Braun, C. Zhang, V. I. Srdanov, A. J. Heeger, G. Stucky, and F. Wudl, Appl. Phys. Lett. **62**, 585 (1993); T. Zukawa, S. Naka, H. Okada, and H. Onnagawa, J. Appl. Phys. **91**, 1171 (2002); S. Shigetomi and T. Ikari, *ibid.* **88**, 1520 (2000).

[26] The current density given at V and T shown in Fig. 1(a) is slightly lower than that at the same V and T in Figs. 2 and 3. This is mainly due to the pulse voltages applied in experiments performed during the 800 IV measurements between the measurements for Figs. 1 and 2.

[27] The determination of the origin of the conductance modulation, i.e., P_S versus charge injection, is not attempted, because several experiments are required to distinguish them even at RT and the determination is more difficult at low T due to the long relaxation time.

[28] R. L. Anderson, Solid-State Electron. **5**, 341 (1962). Some reports claim that the very top surface of PZT is *n* type. Even in this case, the present band diagram is essentially unchanged, because the main effect is the shift of the *pn* boundary in to PZT.

[29] K. W. Böer, Phys. Rev. B **13**, 5373 (1976); V. B. Chougule and S. H. Pawar, Solid State Commun. **48**, 17 (1983).

[30] S. Maniv, M. Shamay, and Y. Sinai, J. Appl. Phys. **62**, 4916 (1987).

[31] If the Z component were due to the avalanche breakdown, we should have seen a substantial increase of the reverse bias current under UV. But, we see none. Additionally, the present reverse bias anomaly is not due to the bulk insulator-conductor transition (see Ref. 32), because the IV curves exhibit well-defined diode characteristics.

[32] Y. Watanabe, J. G. Bednorz, A. Bietsch, Ch. Gerber, D. Widmer, A. Beck, and S. J. Wind, Appl. Phys. Lett. **78**, 3738 (2001).

[33] Y. Watanabe, Phys. Rev. B **57**, 789 (1998); Y. Watanabe, M. Okano, and A. Masuda, Phys. Rev. Lett. **86**, 332 (2001).